High Throughput Screening Reveals Several New Classes of Glutamate Dehydrogenase Inhibitors†

Ming Li, Aron Allen, and Thomas J. Smith*

Donald Danforth Plant Science Center, 975 North Warson Road, St. Louis, Missouri 63132

Received September 13, 2007; Revised Manuscript Received October 23, 2007

ABSTRACT: Glutamate dehydrogenase (GDH) has been shown to play a regulatory role in insulin secretion by pancreatic β-cells. The most compelling evidence of this comes from features of the hyperinsulism/hyperammonemia (HI/HA) syndrome where a dominant mutation causes the loss of inhibition by GTP, and from studies that link leucine (and its analogue BCH) activation of GDH to stimulation of insulin secretion. This suggests that GDH may represent a new and novel drug target to control a variety of insulin disorders. Recently we demonstrated that a subset of green tea polyphenols are potent inhibitors of glutamate dehydrogenase in vitro and can efficaciously block BCH stimulation of insulin secretion. In these current studies, we extend our search for GDH inhibitors using high throughput methods to pan through more than 27,000 compounds. A number of known and new inhibitors were identified with IC_{50}s in the low micromolar range. These new inhibitors were found to act via apparently different mechanisms with some inhibiting the reaction in a positively cooperative manner, the inhibition by only some of the compounds was reversed by ADP, and one compound was found to stabilize the enzyme against thermal denaturation. Therefore, these new compounds not only are new leads in the treatment of hyperactive GDH but also are useful in dissecting the complex allosteric nature of the enzyme.

Mitochondrial GDH[1] (Figure 1) catalyzes the oxidative deamination of L-glutamate and exhibits complex regulation in mammals through inhibition by palmitoyl CoA, GTP, and ATP, and activation by ADP and leucine (*1*). The connection between GDH and insulin regulation was initially established using a nonmetabolizable analogue of leucine (*2*, *3*), BCH (β-2-aminobicycle [2.2.1]heptane-2-carboxylic acid). These studies demonstrated that activation of GDH was tightly correlated with increased glutaminolysis. In addition, it has also been noted that factors that regulate GDH may affect insulin secretion (*4*). It was suggested that glutamate serves as a mitochondrial intracellular messenger when glucose is being oxidized and that the GDH participates in this process by synthesizing glutamate (*5*). However, the hypothesis that GDH, with a very high K_m for ammonium, functions in the reductive amination reaction in vivo is controversial (*6*). Subsequently, it was postulated that glutamine could also play a secondary messenger role and that GDH plays a role in its regulation (*7*−*9*).

The in vivo importance of GDH in glucose homeostasis was demonstrated by the discovery that a genetic hypoglycemic disorder, the hyperinsulinemia/hyperammonemia (HI/HA) syndrome, is caused by dysregulation of GDH (*10*−*12*). Therefore, allosteric regulation of GDH is central to understanding the response of the β-cell to the cellular fuel state. Children with HI/HA have increased β-cell responsiveness to leucine and susceptibility to hypoglycemia following high protein meals (*13*). During glucose-stimulated insulin secretion, it has been proposed that the generation of high energy phosphates inhibits GDH and promotes conversion of glutamate to glutamine which, alone or combined, may amplify release of insulin (*7*, *8*).

In our recent study, we demonstrated that EGCG specifically and allosterically inhibits GDH and, in turn, affects insulin secretion by pancreatic β-cells. Kinetic analysis demonstrated that epigallocatechin gallate (EGCG) and epicatechin gallate (ECG), but not epigallocatechin (EGC) and epicatechin (EC), inhibit purified GDH with nanomolar IC_{50}s (*14*). This inhibition is dependent upon the antenna-like protrusion on the enzyme but is unlikely to bind to the GTP inhibitory site since EGCG inhibits forms of GDH with nonfunctional GTP sites. Studies with pancreatic β-cells demonstrated that EGCG specifically affects insulin secretion under conditions where GDH is known to be important for glucose homeostasis.

In this current study, we have extended the search for new and novel inhibitors of GDH. Of the more than 30,000 compounds tested, a number of new, potent inhibitors were found. However, not all appear to act on GDH in the same manner. Some were found to inhibit the enzyme in a positively cooperative manner. Only in some cases was the inhibition reversed by the allosteric activator, ADP, as was the case with EGCG. Only one compound was found to significantly stabilize the enzyme against thermal denaturation. Therefore, these new compounds not only represent new leads in the treatment of hyperactive GDH found in the HI/HA syndrome but also help to tease out the details of the complex allosteric nature of the enzyme.

† This work was supported by a grant from NIH: DK072171to T.J.S.

* Address correspondence to this author. Tel: 314 587-1451. Fax: 314 587-1551. E-mail: tsmith@danforthcenter.org.

[1] Abbreviations: GDH, glutamate dehydrogenase; EGCG, epigallocatechin gallate; EGC, epigallocatechin; EC, epicatechin; ECG, epicatechin gallate; HCP, hexachlorophene; BSB, 3,3′-[(2-bromo-1,4-phenylene)di(E)ethene-2,1-diyl]bis(6-hydroxybenzoic acid); ATA, aurintricarboxylic acid.

10.1021/bi7018783 CCC: $37.00
Published on Web 11/29/2007

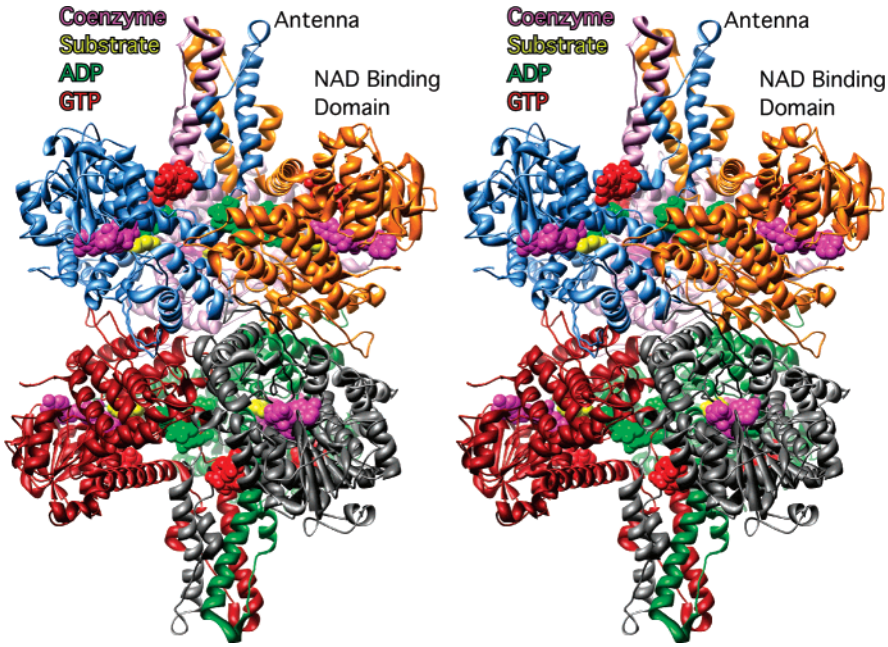

FIGURE 1: The structure of glutamate dehydrogenase. Shown here is a stereo diagram of GDH with the location of some of the various ligands denoted. The subunits of this homohexameric enzyme are represented by ribbon diagrams with differing colors. Coenzyme, glutamate, the inhibitor GTP, and the activator ADP are represented by space filling models colored mauve, yellow, red, and green, respectively. It should be noted, however, that this is a composite structure since ADP and GTP cannot bind simultaneously.

MATERIALS AND METHODS

High Throughput Analysis. The bovine GDH (bGDH) used for these assays was obtained from Sigma Aldrich Chemical Co. as a concentrated stock solution preserved with 50% glycerol. GDH was diluted to a final concentration of 0.06 mg/mL in 0.1 M sodium phosphate buffer, pH 7.5. The substrate mix consisted of 1.6 mM NAD and 100 mM L-glutamate in 0.1 M sodium phosphate buffer, pH 7.5. The stop solution for this reaction was 0.8% sodium dodecyl sulfate in water. Using a Multidrop Combi with stackers (Thermo Labsystems, Franklin, MA), 40 μL of the substrate mix was added to 384 well polystyrene NUNC plates (Nalge Nunc International, Rochester, NY). Using randomly selected libraries of compounds dissolved in DMSO and CyBi-Well pinning robot (CyBio Corp., Jena, Germany), 0.1 μL of each test compound was added to the well. This yielded a final concentration of ~13 μM of test compound and ~0.13% DMSO in the reaction mix after the enzyme was added. The reaction was then initiated by the addition of 20 μL of the enzyme solution and incubated at room temperature for 1 h. The reaction was quenched by the addition of 20 μL of the stop solution, and the plates were read at 360 nm using the Synergy HT (BioTek, Winooski, VT). Normally, NADH production is monitored at 340 nm, but the longer wavelength was used to reduce the interference caused by the polystyrene plates. In the absence of inhibitors, this yielded an OD of ~1.0 and the addition of 0.2% DMSO to the reaction mix had no effect on GDH activity. As a control, 0.2 mM GTP was added and yielded an OD of ~0.1 after the 1 h incubation. When the screen results of the inhibited and uninhibited reactions are compared, the Z' value was calculated to be ~0.87 using eq 1.

$$Z' = \frac{(1 - (3(\mathrm{STD1} + \mathrm{STD2}))}{(\mathrm{MEAN1} - \mathrm{MEAN2})} \qquad (1)$$

Kinetic Analyses. Prior to kinetic analysis, aliquots of GDH were extensively dialyzed against 0.1 M sodium phosphate buffer, pH 7.0, that contained 1 mM EDTA. The enzyme concentration was adjusted to 1 mg/mL and the amount of enzyme added to the reaction mixture was adjusted to yield optimal steady-state velocities. All solutions were made immediately prior to use. Enzyme assays were performed by monitoring reduced coenzyme production at 340 nm using a Beckman Coulter DU800 spectrophotometer.

The IC_{50}s for the top eleven compounds were measured in the oxidative deamination direction in 0.1 M sodium phosphate buffer, pH 8.0, using 50 mM sodium glutamate and 0.2 mM NAD^+. Initially, all of the curves were fitted to a hyperbolic inhibition function:

$$\%\ \mathrm{velocity} = 100\% - \frac{V_i[\mathrm{drug}]}{IC_{50} + [\mathrm{drug}]} \qquad (2)$$

where the V_i is the maximum inhibition caused by the drug (%) and IC_{50} is the concentration of drug that causes half-maximal inhibition of the reaction. As discussed in the results below, the data collected on a number of the compounds did not obey this simple mass action equation and therefore a modified Hill equation (*15*) was applied:

$$\%\ \mathrm{velocity} = 100\% - \frac{V_i[\mathrm{drug}]^h}{IC_{50}{}^h + [\mathrm{drug}]^h} \qquad (3)$$

Here V_i and IC_{50} are as described above and h is the Hill coefficient. Data was fitted using the nonlinear regression routines in the program Prism 4 (GraphPad Software, Inc.).

Analysis of the effects of the various compounds on GDH kinetics is complicated by the fact that the steady-state reaction does not obey Michaelis−Menten behavior when either glutamate or coenzyme is varied in the reaction. When $NAD(P)^+$ is varied in the oxidative deamination reaction,

there is pronounced negative cooperativity. Therefore, the velocities of the reaction at varied NAD^+ and drug concentrations were analyzed using the Hill equation:

$$\text{velocity} = \frac{V_{max}[NAD^+]^h}{K_{0.5}{}^h + [NAD^+]^h} \quad (4)$$

Here, V_{max} is the maximum velocity of the reaction and h is the Hill coefficient. Note that that the $K_{0.5}{}^h$ term is not the same as a K_m value. The data was directly fitted to this equation using the nonlinear regression algorithms in the program Prism 4.

In the case of glutamate-varied analysis, there is strong substrate inhibition at high glutamate concentrations. For this equation, a modified version of the Monod equation was used (*16*):

$$\text{velocity} = \frac{V_{max}[GLU]}{K_m + [GLU] + [GLU]^2/K_i} \quad (5)$$

Here V_{max} is the apparent maximum velocity in the absence of substrate inhibition, K_m is the apparent Michaelis constant for glutamate, and K_i is the apparent substrate inhibition coefficient. It should be noted, however, that this is an empirical description of the inhibition of the reaction at high glutamate concentrations. Equation 5 is a derivative of that for an uncompetitive inhibitor, and therefore inhibition is caused by the binding of a second substrate molecule after the first molecule is bound to the active site. In the case of GDH, substrate inhibition is due to the binding of glutamate to the active site before the reduced coenzyme disassociates from the prior turnover event (*17*). Further, the binding of NAD(P)H from the GDH·GLU·NAD(P)H is much tighter than of the GDH·αKG·NAD(P)H complex. Therefore, eq 5 reflects the concentration dependency of the glutamate inhibition but does not fully describe its complexity. Nevertheless, while the K_i values determined using this equation do not truly represent the K_i for glutamate inhibition, they are useful in ascertaining whether the drugs affect overall substrate inhibition and help remove the effects of substrate inhibition from the curve fitting results at lower glutamate concentrations.

ADP Activation Studies. ADP activation is highly dependent upon pH and substrate concentrations (*18*) and is efficacious at allosterically abrogating the effects of inhibitors such as EGCG (e.g. (*14*)). To delineate possible differences in the mode of action of the various inhibitors, the ability of ADP to reverse the inhibition caused by these compounds was examined. For these assays, 10 μL of a 1 mg/mL solution of GDH was added to 1 mL cuvettes containing 25 mM L-glutamate, 0.2 mM NAD^+ in 0.1 M sodium phosphate buffer, pH 8.0 and the production of NADH was monitored spectrophotometrically at 340 nm. Since the compounds inhibited the reaction to varying degrees, the data for each were also graphed as percentage of activity in the absence of ADP. The data was then analyzed using the formula

$$\%\ \text{activity} = 100 + \frac{\text{Act}_{max}[ADP]}{(K_{act} + [ADP])} \quad (6)$$

where K_{act} is the apparent binding constant associated with the ADP activation and Act_{max} is the maximum amount of activation of the reaction caused by ADP.

Binding Studies. At an excitation wavelength of 365 nm, BSB has an emission maximum at 520 nm. Upon the addition of enzyme, the fluorescence is enhanced and blue-shifted to 475 nm. Therefore for binding experiments, the excitation wavelength was 365 nm and the emission wavelength was 475 nm. The binding equilibrium constant was measured by monitoring the change in fluorescence. Because of limited solubility, the concentration of BSB was fixed and GDH was added to the cuvette. The GDH had been extensively dialyzed against 0.1 M sodium phosphate buffer, pH 7.0, that contained 1 mM EDTA and the protein concentrations were adjusted to the noted final concentrations assuming an extinction coefficient of 0.93 mL/cm·mg. BSB binding was measured fluorometrically by successive additions of GDH to the same cuvette, and the fluorescence intensity was recorded after each addition. Fluorescence intensity was measured using a Cary Eclipse fluorometer with excitation and emission slit widths set to 5 nm, and each fluorescence reading was averaged over 0.1 s. The problem with this experimental design was the fact that the initial additions of GDH were nearly all saturated with ligand. Therefore, the data was analyzed using a modified version of previously described equation (*19*) that does not assume that the bound enzyme concentration is negligible compared to the total enzyme pool:

$$F = F_{max}\frac{-b - \sqrt{b^2 - 4a[GDH]}}{2a} + F_0 \quad (7)$$

where

$$b = -(K_d + [drug]_{tot} + [GDH])$$

$$a = [drug]_{tot}$$

In this equation, F_0 is the initial fluorescence of the compound before GDH is added, $[drug]_{tot}$ is the initial concentration of drug in the cuvette, and F_{max} is the fluorescence of the drug after it has all bound to GDH. The data was fit to the above equation using the program Prism.

Isothermal Titration Calorimetry (ITC). ATA binding assays were performed using ~7 μM samples of bGDH that had been dialyzed against 100 mM sodium phosphate buffer, pH 7.0. ITC measurements were carried out on a MicroCal VP-ITC titration calorimeter (MicroCal, Inc., Northampton, MA). The protein samples were placed in the reaction cell, and a 2.0 mM solution of ATA was used in the injection syringe.

All titrations were performed at 30 °C. After the temperature was equilibrated, successive injections of ATA were made into the reaction cell in 10 μL while stirring at 260 rpm to ensure a complete equilibration. The resulting heat of reaction was measured in 29 consecutive injections at 400 s time intervals. Control experiments to determine the heat absorbed due to dilution of the ATA solution were carried out with identical injections in the absence of protein. These values were then used to normalize the binding data. The titration data were curve-fitted to models that assumed either one or two classes of non-interacting binding sites using a nonlinear least-squares algorithm in the MicroCal Origin

software package. The binding enthalpy change ΔH, association constant K_a, and the binding stoichiometry n were all refined during the least-squares minimization process. For this fitting process, an accurate measure of ligand concentration is required. However, ATA is notorious for being a mixture of different polymeric states. In order to obtain a quality fit of a single site model to the data, it was necessary to adjust the apparent concentration of ATA down to 0.24 mM.

Thermal Denaturation Studies. The effects of the various compounds on GDH thermal stability were assayed at 50 °C and 54 °C depending upon the compound being analyzed. A 1 mg/mL solution of GDH in 0.1 M sodium phosphate, pH 7.0, was incubated in the presence of 0.1 mM drug at the noted temperatures. At varying times, 10 μL of this mixture was removed and the activity of the enzyme was measured in 1 mL cuvettes containing 25 mM sodium L-glutamate, 0.2 mM NAD^+ in 0.1 M sodium phosphate buffer, pH 8.0, and the production of NADH was monitored spectrophotometrically at 340 nm. At this concentration of drug, some of the compound was carried over from the incubation aliquot and caused inhibition of the enzymatic reaction. Therefore, the data was normalized to the enzymatic activity before heat treatment and analyzed using least-squares fitting to a simple exponential decay formula:

$$\% \text{ activity} = 100\, e^{-Kt} \quad (8)$$

where K is the decay constant and t equals time.

RESULTS

The hyperinsulinism/hyperammonemia syndrome (HI/HA) is directly caused by the hyperactivity of GDH that stems from genetic defects that abrogate GTP inhibition. The overriding goal here is to find novel compounds that may ameliorate some of these symptoms by modulating the hyperactive GDH in these patients. To this end, the assay was designed to look for inhibitors of the oxidative deamination reaction. To eliminate possible molecular mimics of the substrate or coenzyme, the assay was performed at high glutamate and NAD concentrations at a pH where their binding is strongest (pH 8.0). Further, it is at these conditions that other known allosteric inhibitors (e.g., GTP) exhibit their highest activity.

Using the high throughput screening facilities at the Broad Institute, approximately 27,000 compounds were tested for the ability to inhibit GDH activity. Each assay was performed in duplicate with DMSO controls on each plate in addition to control plates composed entirely of DMSO. The raw data was processed using the in-house services at the Small Molecule Screening Center at the Broad Institute. Figure 2 is a scatter plot of the Zscore from each of the duplicate assays. In this inhibition assay, "hits" should have large negative composite scores. It should be noted that the data also splays in the positive direction along the X and Y axes and that there are a significant number of compounds with high positive composite Zscores. Both effects are more than likely due to two sources of artificially high OD readings; the SDS stop solution occasionally formed bubbles in the well that scatter light, and some of the tested compounds absorb strongly at 360 nm. Indeed, a number of these

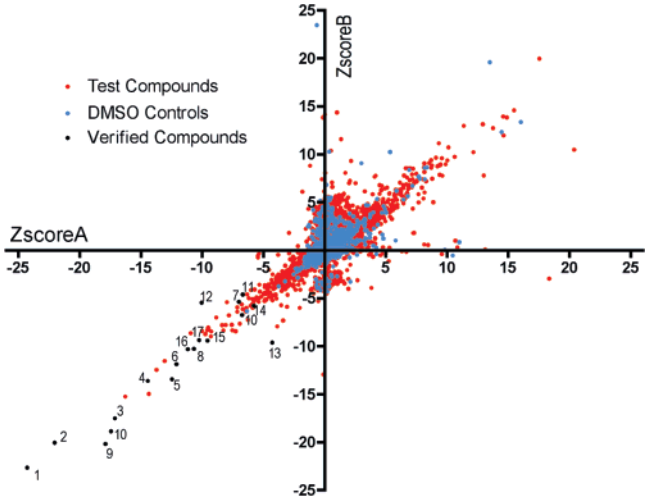

FIGURE 2: High throughput screening for glutamate dehydrogenase inhibitors. The effect of each compound on GDH activity was measure in duplicate and plotted here as a function of the two Zscore values. The DMSO controls are represented by blue dots, the red dots represent the test compounds, and the black dots represent those that were further analyzed in these studies. The numbering used to identify the black dots corresponds to the compound identification used in Figure 2.

compounds were further examined using the 1 mL cuvette assay, and none were shown to activate the reaction.

Figure 3 shows a summary of the activity of a number of the compounds identified in the high throughput screen. It is important to note that some known inhibitors of GDH were also found to be potent inhibitors in this high throughput screen. Most notably, diethylstilbestrol, epigallocatechin-3-monogallate (EGCG) and a digallate derivative were found to be potent inhibitors. Furthermore, and as we had previously found, epicatechin (EC) was not active against GDH (*14*). At first glance, it appears that polyaromatic compounds have the highest activity. However, there are apparently other important factors governing activity since compounds such as epigallocatechin (EGC) and EC did not exhibit activity while the closely related epicatechins (EGCG, epicatechin-3-monogallate, and epigallocatechin 3,5-digallate) did. As shown in Figures 2 and 3, there is a general agreement between the composite Zscore for the compounds and the strength of the inhibition in the 1 mL assays. It should be noted that there are still a number of hits shown in Figure 2 that have not yet been confirmed with traditional kinetic assays and will be the subject of future studies.

While the estimated IC_{50} values are summarized in Figure 3, the details of the dose-dependent inhibition are shown in Figure 4 and summarized in Table 1. When the data was analyzed using the simple hyperbolic equation 2, it was immediately apparent that most of these compounds do not exhibit a simple pattern of dose-dependent inhibition. As shown in the expanded view in Figure 4, the inhibition of some of the compounds had a sigmoidal shape that was indicative of positive cooperativity. When the modified Hill equation was used instead (eq 3), the data was well represented by the fitted curve. Approximately half of the compounds had Hill coefficients of ~1.0 and therefore did not exhibit any apparent cooperativity. However, ATA, HCP, bithionol, metergoline, calmidazolium, and BH3I all had Hill coefficients much larger than 1.0 and significantly sigmoidal

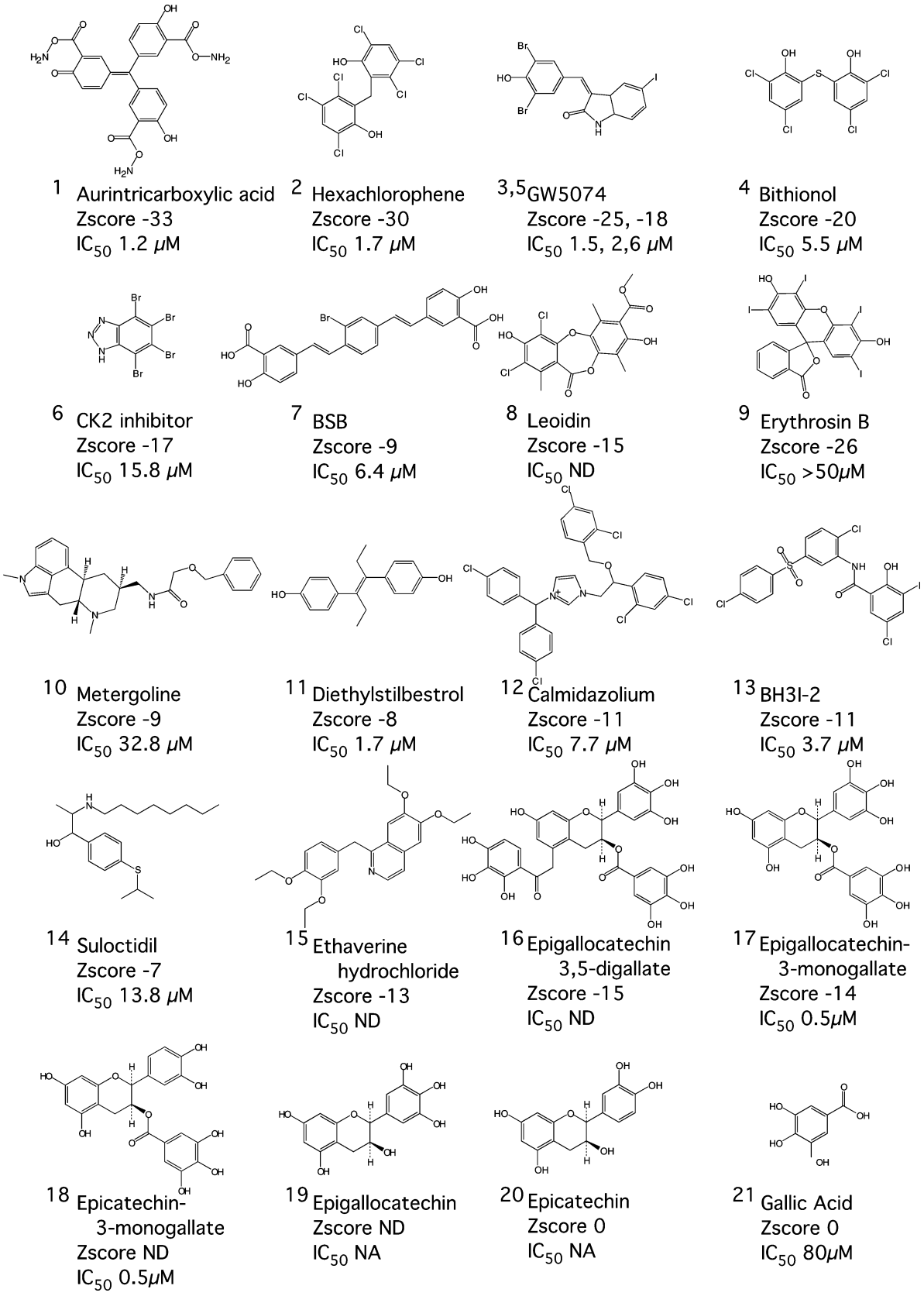

FIGURE 3: Structures and activities of some of the compounds tested against GDH. Shown here are a number of the newly identified inhibitors against GDH as well as previously published work with their associated overall Zscore and IC_{50} values.

shaped dose-dependency curves. This suggests that these compounds do not all have the same effect on GDH. It should be noted that, as evidence for the quality of the curve fitting process, the maximum inhibition for all of the compounds was allowed to vary during the fitting process and, in all cases, inhibition was ~100%.

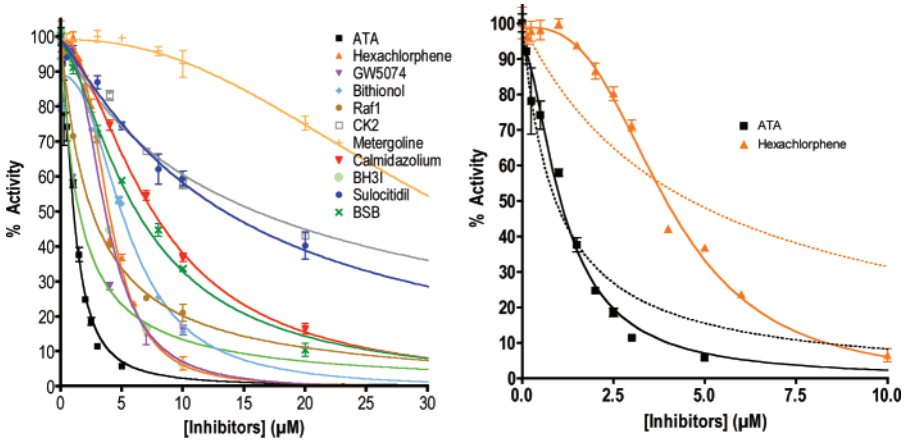

FIGURE 4: The dose dependent inhibition of GDH activity by the top eleven compounds identified in the high throughput screen. Shown here is the dose dependent inhibition of GDH activity for the best compounds identified in the high throughput screen. The lines represent the results of nonlinear least-squares fitting using a modification of the Hill equation (eq 3). On the right is an expanded view of two of the active compounds showing that fitting the data to a simple hyperbolic function (dashed line) does not sufficiently describe the dose-dependent inhibition.

Table 1: Summary of the Nonlinear Curve Fitting Results of the Various Compounds Using the Modified Hill Equation (Eq 3)[a]

compound	I_{max} (%)	K_i (μM)	Hill coefficient	R^2	pharmaceutical target
ATA	94 (3.1)	1.1 (0.09)	1.7 (0.19)	0.97	nuclease inhibitor (*28*)
hexachlorophene	99 (1.1)	4.0 (0.08)	2.9 (0.17)	0.99	topical antiseptic
GW5074	100 (2.1)	1.5 (0.13)	0.98 (0.07)	0.99	cRaf1 kinase inhibitor (*50*)
cRaf1 Inhibitor	100 (1.3)	2.6 (0.12)	0.99 (0.04)	1.00	cRaf1 kinase inhibitor (*50*)
bithionol	89 (3.4)	5.5 (0.37)	2.4 (0.38)	0.95	antihelmintic, fungicidal
CK2 Inhibitor	101 (2.0)	16. (1.1)	0.89 (0.06)	0.99	ATP/GTP-competitive inhibitor of casein kinase-2 (*31*, *51*)
metergoline	99 (2.3)	33. (3.0)	2.3 (0.36)	0.94	serotonin receptor antagonist (*40*)
calmidazolium	98 (1.7)	7.7 (0.22)	1.7 (0.08)	1.00	inhibitor of calmodulin-regulated enzymes (*52*)
BH3I	99 (2.5)	3.7 (0.09)	2.5 (0.13)	1.00	blocks BH3 domain and Bcl-xL interaction (*34*)
sulocitidil	99 (1.1)	14. (0.83)	1.1 (0.10)	0.98	calcium channel blocker (*53*), anticoagulant, vasodilator
BSB	98 (1.5)	6.4 (0.32)	1.5 (0.11)	0.99	binds to amyloid plaques (*32*)

[a] The values in parentheses denote the standard error of the fitted parameters.

These results suggested that all of the compounds are not inhibiting GDH in the same manner. To further analyze this, several of the more potent compounds were selected for further steady-state analysis. These studies are shown in Figure 5 and summarized in Tables 2 and 3. To complicate this analysis is the fact that GDH does not follow the expected Michaelis−Menten behavior. In the oxidative deamination reaction, high glutamate concentrations cause substrate inhibition (*18*) and there is marked negative cooperativity when $NAD(P)^+$ is varied in the steady-state reaction (*20*−*23*). Rather than trying to ascertain the effects of the drugs using rather narrow concentration ranges of coenzyme and substrate, the data was analyzed using nonlinear regression analysis.

For analysis of the steady-state reaction at varied coenzyme concentration (Figure 5A, C, E), a modified version of the Hill equation was used (eq 4). It should be noted, however, that the $K_{0.5}{}^h$ values for NAD are higher than previously published K_m values under similar conditions (e.g., (*18*)). This is likely due to the fact that the two apparent binding constants are not mathematically equivalent. One problem with the Hill equation is that a small change in the Hill coefficient has an exponential effect. To help compensate for this, all of the data was curve-fitted at the same time while globally fitting the Hill coefficient. This, in fact, yielded better R^2 values for fitting than when the Hill coefficient was refined independently for each data set. This suggests that none of the three compounds affect the subunit communication that is responsible for negative cooperativity. BSB yielded the clearest results in that increasing concentrations of the drug decreased the V_{max} and the K_m for the reaction. HCP also clearly decreased the V_{max} for the reaction but the effects on the K_m for NAD^+ are less clear. At the highest drug concentration, HCP also appears to decrease both the K_m and the V_{max} for the NAD^+ varied steady-state reaction. The results for ATA are similar to those with HCP. Nevertheless, it is highly unlikely that these compounds act as competitive inhibitors to coenzyme.

The steady-state kinetic analysis of the glutamate-varied reaction also suggests that these compounds are not affecting the enzyme in the same manner (Figures 5B, D, and F). The initial velocity for the reaction is significantly inhibited at high glutamate concentrations, and therefore a modified version of the Monod equation was used (*16*) for analysis (eq 5). For the nonlinear regression analysis, the apparent binding constant for the substrate inhibition (K_i in eq 5) was allowed to vary for each dataset and was also globally refined to a single value. The constrained refinement yielded superior R^2 values for the curve fitting process. From this, it is apparent that the substrate inhibition is essentially unaffected by the compounds. However, from the results of the analysis (Table 3), it appears that the larger, polymeric compounds, ATA and BSB, increase the K_m for glutamate while the smaller, hydrophobic, hexachlorophene either does not affect the K_m for glutamate or causes a slight decrease. This effect is further examined in Figure 6. For this figure, the velocities

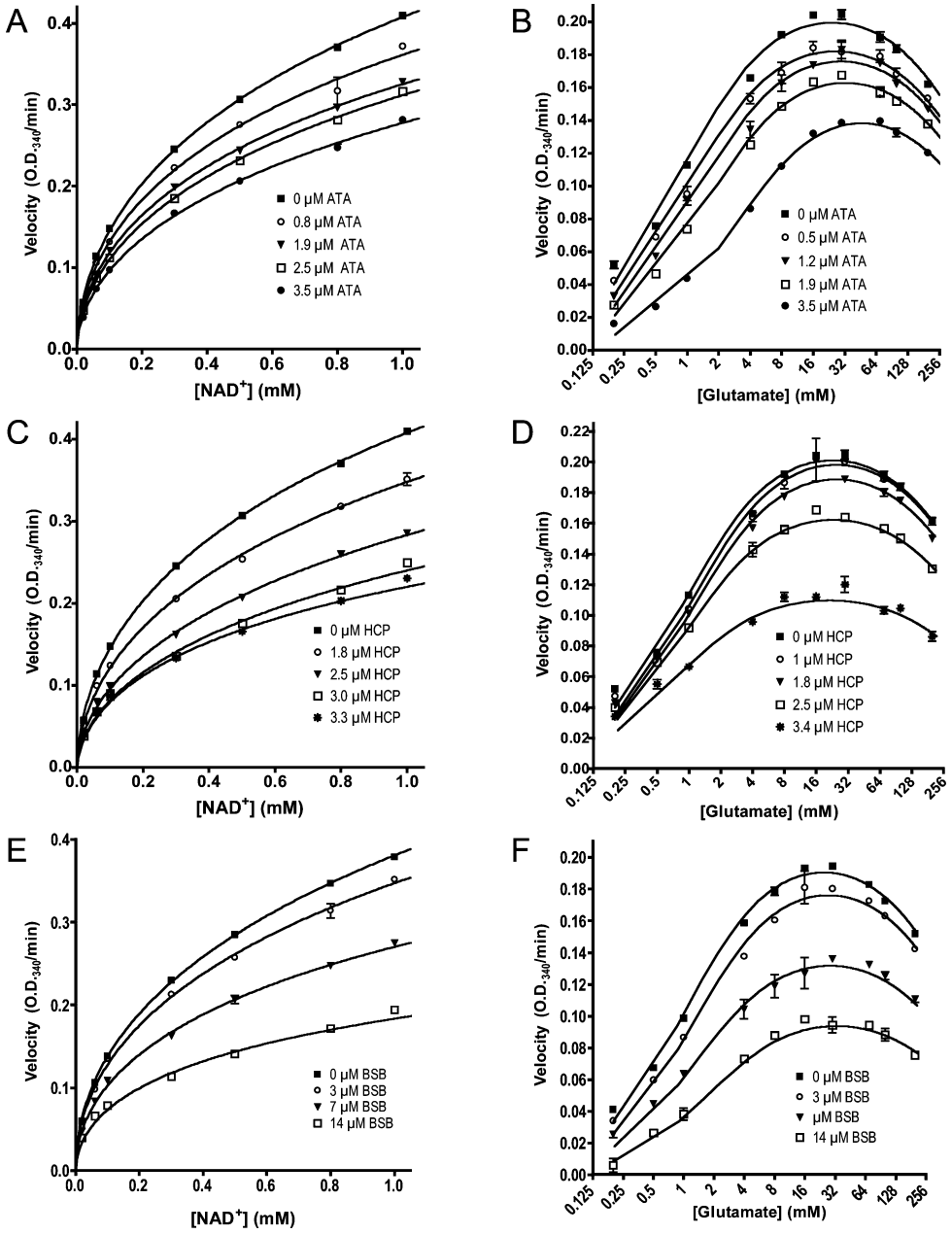

FIGURE 5: Effects of several of the more potent drugs on glutamate and coenzyme varied steady-state kinetics of the oxidative deamination reaction. The figures on the left side of this page represent steady-state velocities at varied coenzyme concentration, and the figures on the right are of the glutamate varied studies. The effects of ATA, HCP, and BSB are shown in the top, middle, and bottom figures, respectively. The data for the coenzyme varied experiments were fitted to the modified Hill equation (eq 4) while the modified Monod equation (eq 5) was used to describe the substrate inhibition observed in the glutamate varied studies.

of the reactions at the highest drug concentration were compared to the velocities of the reactions in the absence of drug. From this figure, it is apparent that ATA and BCB are less effective at higher glutamate concentrations. This, combined with the fact that these drugs increase the K_m for glutamate, suggests an antagonism between these drugs and glutamate. This is not the case for coenzyme (Table 2). In contrast, hexachlorophene appears to be more efficacious as the glutamate concentration is increased. From these results, it appears that ATA and BSB disrupt the GDH·NAD^+·GLU complex while hexachlorophene promotes its formation. In the case of the latter, it may be that, like GTP, hexachlorophene promotes the formation of the abortive complex (GDH·NADH·GLU).

ATA and BSB tend to form larger polymers in solution and, from their action on other targets, appear to bind to large oligomers. Therefore, there was some concern as to the specificity of their interactions with GDH. To that end, binding studies were performed on both ATA and BSB. Both molecules are fluorescent and therefore were first analyzed using fluorescence titration experiments. ATA was found to not be suitable since it, by itself, tends to exhibit enhanced fluorescence in a concentration dependent manner. BSB binding followed classic saturation behavior, and the data was well described by the modified saturation formula (Figure 7, eq 7). The K_d for the interaction was calculated to be 1.5 μM ($\pm$0.4 μM), and the R^2 for the fitting process was 1.00. This binding constant is within an order of

Table 2: The Effects of the Inhibitors on the Oxidative Deamination Reaction at Varying Coenzyme Concentrations[a]

	[ATA]				
	0 μM	0.8 μM	1.9 μM	2.5 μM	3.5 μM
V_{max} (OD_{340}/min)	1.90 (0.31)	1.49 (0.22)	1.37 (0.22)	1.54 (0.31)	1.52 (0.37)
Hill coefficient	0.52 (0.011)	0.52 (0.011)	0.52 (0.011)	0.52 (0.011)	0.52 (0.011)
$K_{0.5}{}^h$ for NAD^+ (mM)	11.9 (5.2)	8.9 (3.6)	9.3 (4.0)	14.0 (7.2)	17.8 (10.6)
R^2	1.00	0.99	1.00	1.00	1.00
	[HCP]				
	0 μM	1.8 μM	2.5 μM	3.0 μM	3.3 μM
V_{max} (OD 340/min)	1.90 (0.31)	1.83 (0.37)	1.81 (0.51)	1.43 (0.41)	0.87 (0.16)
Hill coefficient	0.52 (0.011)	0.52 (0.011)	0.52 (0.011)	0.52 (0.011)	0.52 (0.011)
$K_{0.5}{}^h$ for NAD^+ (mM)	21.5 (17.0)	16.0 (8.4)	25.3 (17.3)	21.3 (14.6)	7.7 (3.6)
R^2	1.00	1.00	1.00	1.00	1.00
	[BSB]				
	0 μM	3.0 μM	7.0 μM	14.0 μM	
V_{max} (OD_{340}/min)	1.62 (0.25)	1.35 (0.19)	0.92 (0.12)	0.52 (0.067)	
Hill coefficient	0.52 (0.011)	0.52 (0.011)	0.52 (0.011)	0.52 (0.011)	
$K_{0.5}{}^h$ for NAD^+ (mM)	9.7 (4.1)	7.8 (3.0)	5.4 (2.0)	3.0 (1.1)	
R^2	1.0	1.0	1.0	1.0	

[a] This is a summary of the data shown in Figure 5 and fitted to eq 4. For this analysis, the Hill coefficient was refined globally to a single value using all of the datasets. Note that the $K_{0.5}{}^h$ term is not the same as a K_m value.

Table 3: The Effects of the Inhibitors on the Oxidative Deamination Reaction at Varying Glutamate Concentrations[a]

	[ATA]				
	0 μM	0.8 μM	1.9 μM	2.5 μM	3.5 μM
V_{max} (OD_{340}/min)	0.22 (0.002)	0.20 (0.002)	0.19 (0.002)	0.18 (0.002)	0.16 (0.003)
K_m (mM)	0.89 (0.05)	0.99 (0.06)	1.2 (0.07)	1.5 (0.10)	3.0 (0.23)
K_i	696(45)	696(45)	696(45)	696(45)	696(45)
R^2	0.99	0.99	0.99	0.99	0.99
	[HCP]				
	0 μM	1.0 μM	1.8 μM	2.5 μM	3.4 μM
V_{max} (OD_{340}/min)	0.22 (0.002)	0.21 (0.002)	0.20 (0.002)	0.18 (0.002)	0.12 (0.002)
K_m (mM)	0.89 (0.05)	0.98 (0.05)	0.96 (0.05)	0.81 (0.05)	0.65 (0.06)
K_i	595 (37)	595 (37)	595 (37)	595 (37)	595 (37)
R^2	0.99	0.99	0.98	0.99	0.96
	[BSB]				
	0 μM	3.0 μM	7.0 μM	14.0 μM	
V_{max} (OD_{340}/min)	0.21 (0.002)	0.19 (0.002)	0.14 (0.002)	0.11 (0.002)	
K_m (mM)	1.0 (0.06)	1.2 (0.06)	1.3 (0.10)	1.7 (0.19)	
K_i	598(45)	598(45)	598(45)	598(45)	
R^2	0.99	0.99	0.98	0.98	

[a] This is a summary of the data shown in Figure 5 and fitted to eq 5. For this analysis, the apparent substrate inhibition binding constant (K_i) was refined globally to a single value using all of the datasets.

magnitude of the K_i measure by steady-state analysis (Table 1). ATA is more soluble than BSB and therefore amenable to other methods for measuring binding constants such as isothermal calorimetry titration. As shown in Figure 8, ATA binding also showed classical saturation binding with a calculated binding constant of 4.1 μM. This is consistent with the K_i measured kinetically. In both cases, the binding was well described by a single site, non-interacting binding model as apposed to the apparent positive cooperative effect observed in the steady-state analysis (Figure 4). This suggests that the drug binding to the enzyme alone is different than binding to the catalytic complex. Nevertheless, these binding experiments demonstrate that these compounds do indeed bind in a specific manner with association constants consistent with the measured kinetic ED_{50}s.

ADP activation is very sensitive to pH and the concentration of coenzyme and substrate (*18*). For example, ADP can actually inhibit the oxidative deamination reaction at pH 6.0 (*18*). In vivo, it seems likely that ADP functions largely to attenuate the effects of inhibitors such as palmitoyl CoA and GTP. To help tease out possible differences in the mode of action of the various compounds, the effects of ADP on these inhibitors were analyzed. Figure 9 displays this data two different ways. On the left are the raw velocity measurements as the concentration of ADP is increased. Notably, the velocities at 0 μM ADP differ because the activity of the drugs varies widely. The data is also plotted as a function of percent activity in the absence of ADP. This helps to normalize the various experiments so that the ADP abrogation of drug inhibition could be directly

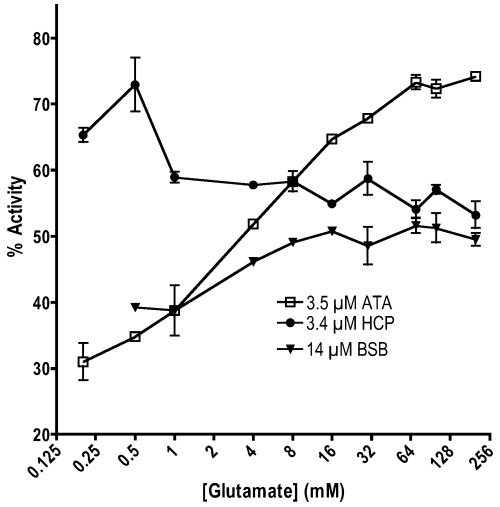

FIGURE 6: The effects of glutamate concentrations on GDH inhibition. Shown here is a summary of Figures 5 B, D, and F as the percent GDH activity at the highest concentrations of ATA, HCP, and BSB as the concentration of glutamate is increased.

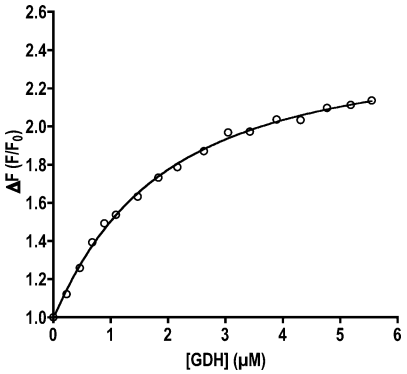

FIGURE 7: Fluorescence binding analysis of BSB. Shown here is the change in fluorescence of BSB as the concentration of GDH is increased. The line represents the curve fitting results using eq 8.

compared. The nonlinear regression analysis is summarized in Table 4.

There appears to be a continuum with regard to ADP abrogation of drug inhibition. At either end of this spectrum are ATA and GW5074. Both of these compounds are potent inhibitors of GDH, and sufficient amounts of drug were added to inhibit the reaction by nearly 75%. As summarized in Table 4, at this concentration, ATA increases the K_{act} of ADP by 10-fold and the apparent maximum activation also by about 10-fold. Or, to put it another way, ADP is very efficacious at removing ATA inhibition, and from extrapolation, it seems that ADP could nearly remove ATA inhibition at high enough concentrations. The ADP concentrations shown here are at the limit of what can be used since at higher concentrations it starts to compete with coenzyme for the active site. This is very much the same as what we observed in the case of EGCG (*14*). In stark contrast to ATA, GW5074 is relatively unaffected by ADP. Using the more reliable curve fitting results at 8 μM GW5074, the apparent binding constants of, and the extent of activation by, ADP are essentially the same as they are in the absence of drug. Other than perhaps DES, the other compounds seem to be more akin to ATA than GW5074 in that their inhibitory effects all seem to be well reversed by ADP. Any more subtle

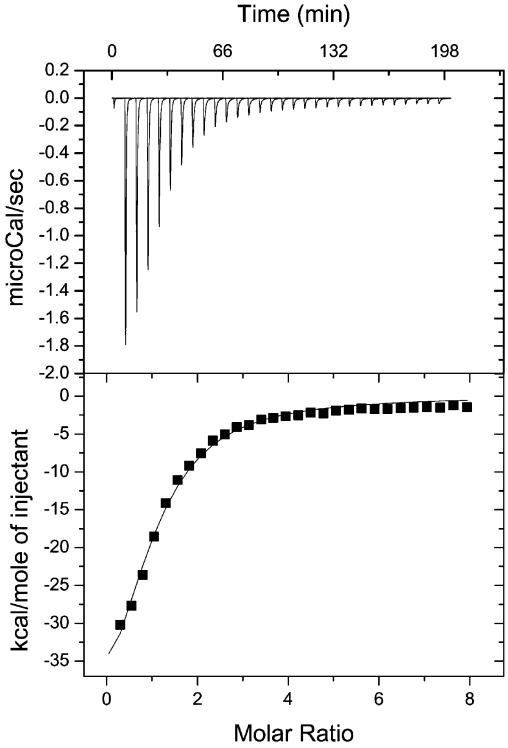

FIGURE 8: Isothermal calorimetry titration analysis of ATA binding. Shown here are the ITC results of ATA binding to GDH. The top figure shows the raw data, and the figure at the bottom shows the summary of the data along with the curve fitting results.

differences among these compounds may be more due to efficacy rather than mode of action.

The NAD binding domain of GDH undergoes a large conformational change during catalytic turnover. Previously we suggested that allosteric regulation is exacted through control of this motion (*24*, *25*). In other studies, we have shown that antiviral drugs to human rhinovirus act by stabilizing the virion and preventing conformational changes (*26*, *27*). Therefore, the effects of these drugs on GDH thermal stability were examined (Figure 10). This figure shows the data in terms of raw velocity (top) and as a percentage of activity before heat treatment (bottom). The initial velocity is lower with some drugs because some drug is carried over from the high temperature incubation to the enzymatic assay. From preliminary studies, ATA was found to stabilize GDH and therefore the assay was also performed at a slightly higher temperature to exemplify this (right side of Figure 10). The effects of the drugs on the rate of denaturation are summarized in Table 5. Contrary to our initial hypothesis, many of the compounds caused a marked destabilization of GDH. The most potent of these compounds are DES and palmitoyl CoA. These compounds increased the sensitivity of GDH to thermal denaturation by nearly a factor of 10. Calmidazolium and hexachlorophene had little to no effect on GDH stability and may have slightly stabilized the enzyme. Most of the other compounds affect the half-life of GDH by about a factor of 2. ATA is very different than all of the other compounds in that it increases the stability of GDH by approximately 4-fold. Consistent with the other experiments, these results strongly imply that these compounds are not acting via the same mechanism.

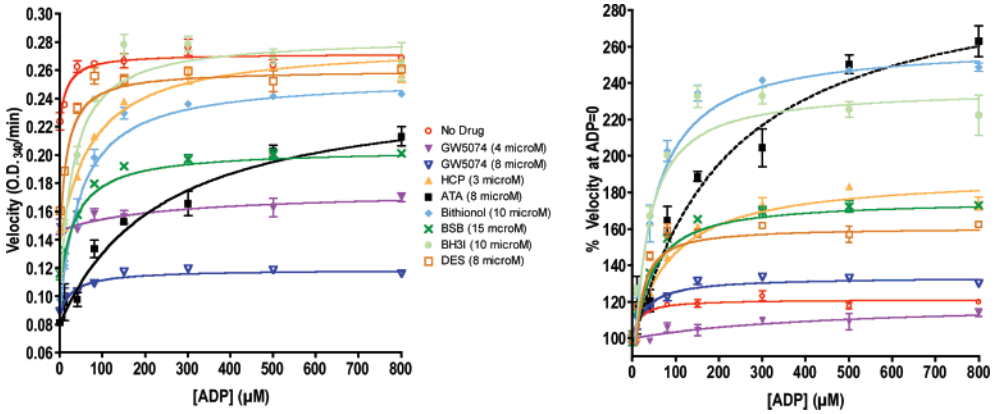

FIGURE 9: Effects of ADP on the inhibition of the various compounds. On the left is the raw data showing the effects of ADP on the velocity of the GDH catalyzed oxidative deamination reaction. On the right, the same data has been normalized and presented as a percentage of the velocity at zero ADP concentrations. The curves shown in this figure are the results of nonlinear regression analysis using eq 6.

Table 4: ADP Reversal of Inhibition of the Various Compounds[a]

compound	[drug] (μM)	activation (%)	K_{act} ADP (μM)	R^2
no drug		21 (1.3)	17 (6.2)	0.88
GW5074	4	21 (9.4)	449 (411)	0.71
GW5074	8	34 (2.0)	31 (9.2)	0.90
hexachlorophene	3	92 (4.4)	89 (15)	0.97
ATA	8	207 (17)	222 (49)	0.96
bithionol	10	164 (4.7)	51 (6.2)	0.98
BSB	15	79 (1.8)	41 (32)	0.99
BH3I	10	140 (5.9)	34 (7.0)	0.95
DES	8	64 (2.0)	19 (3.4)	0.96

[a] Shown here is a summary of the data shown in Figure 9, fitted to eq 6.

DISCUSSION

Hyperinsulinism/hyperammonemia in humans is associated with dysregulation of GDH (*10*−*12*). The mutations leading to this phenotype either directly alter the GTP binding site or appear to affect the ability of this inhibitor to exert its effects. Our previous studies demonstrated that some of the polyphenols found in green tea are able to inhibit both the wild type and HI/HA forms of GDH in vitro as well as block the GDH mediated process of BCH stimulation of insulin secretion in situ. It was clear from these studies that the observed inhibition was specific to EGCG and ECG and independent of the antioxidant activity of these compounds (*14*). However, while these compounds are safe for consumption, they are cleared from the serum in relatively short order. Therefore, the current studies were undertaken to identify inhibitors that might have superior pharmokinetics and to identify a cluster of active compounds for quantitative structure−activity relationships. Along the way, it was hoped that such analysis would tease out the mechanisms of regulation in this complex enzyme.

Of the most active compounds, a number of them have similar known pharmaceutical activities. It should be noted that none of the compounds either aggregated or disrupted this hexameric enzyme according to dynamic light scattering experiments (data not shown). The first group of active compounds likely inhibits GDH by interacting with one of the several purine binding sites (ADP, GTP, or coenzyme binding sites). Aurintricarboxylic acid (ATA) is an inhibitor of nucleases (*28*) and topoisomerases (*29*) and has been shown to inhibit protein−nucleic acid interactions (*30*). From the structure (Figure 3), it is not clear what aspect of the compound might be mimicking purines and pyrimidines. CK2-inhibitor is a cell-permeable and highly selective ATP/GTP competitive inhibitor of casein kinase-2 (*31*). Against this target, it has a K_i of ∼1 μM and likely has activity due to its similarity to a purine ring. GW5074 is a c-Raf1 inhibitor with an EC_{50} of ∼10 nM. Similar to the CK2 inhibitor, this compound is probably active due to the purine analogue at the one end (Figure 3).

A second group of active compounds act on their targets by binding to protein−protein interfaces. BSB is able to permeate living cells, cross the blood−brain barrier, and bind to intracellular amyloid peptides associated with Alzheimer's disease (*32*). In addition, BSB was shown to inhibit a cellular model for transmissible spongiform encephalophathy with an ED_{50} of ∼1.4 μM (*33*). BH3I-2 inhibits the interaction between the BH3 domain and Bcl-xL (*34*) with a K_i of ∼4−6 μM. It is tempting to speculate that these compounds might interfere with the large domain motion associated with catalytic turnover by binding to, for example, the back of the NAD binding domain (Figure 1).

Interestingly, a number of these GDH inhibitors also have activity on systems related to calcium binding and uptake. Ethaverine is structurally related to verapamil, and both are L-type calcium channel inhibitors (*35*). However, verapamil did not significantly inhibit GDH activity in this screen (data not shown). Suloctidil is also a calcium channel blocker (*36*) that also can inhibit caspase-3 (*37*). Calmidazolium is a calmodulin antagonist that has a number of activities including the inhibition of calcium channels (*38*), and calcium-dependent kinases (*39*). It is not at all clear what the GDH might have in common with calcium channels.

The remaining compounds have a wide range of pharmaceutical activities, but all are polyaromatics. Metergoline is a nonselective serotonin receptor antagonist, known to have an effect on 5HT1A, 5HT1D and 5HT2C receptors (*40*, *41*). Diethylstilbestrol is a synthetic nonsteroidal substance with estrogenic properties (*42*) and used in the treatment of prostatic cancer. Hexachlorophene and the very similar bithionol both have general bactericidal and fungicidal activity, but their exact mechanism of action is unknown. Finally, the catechins are polyphenolic compounds with strong antioxidant activity. However, inhibitory activity against GDH is limited to ECGC and ECG and apparently unrelated to the antioxidant activity. Interestingly, gallate is not at all active and yet hexachlorophene and bithionol, with

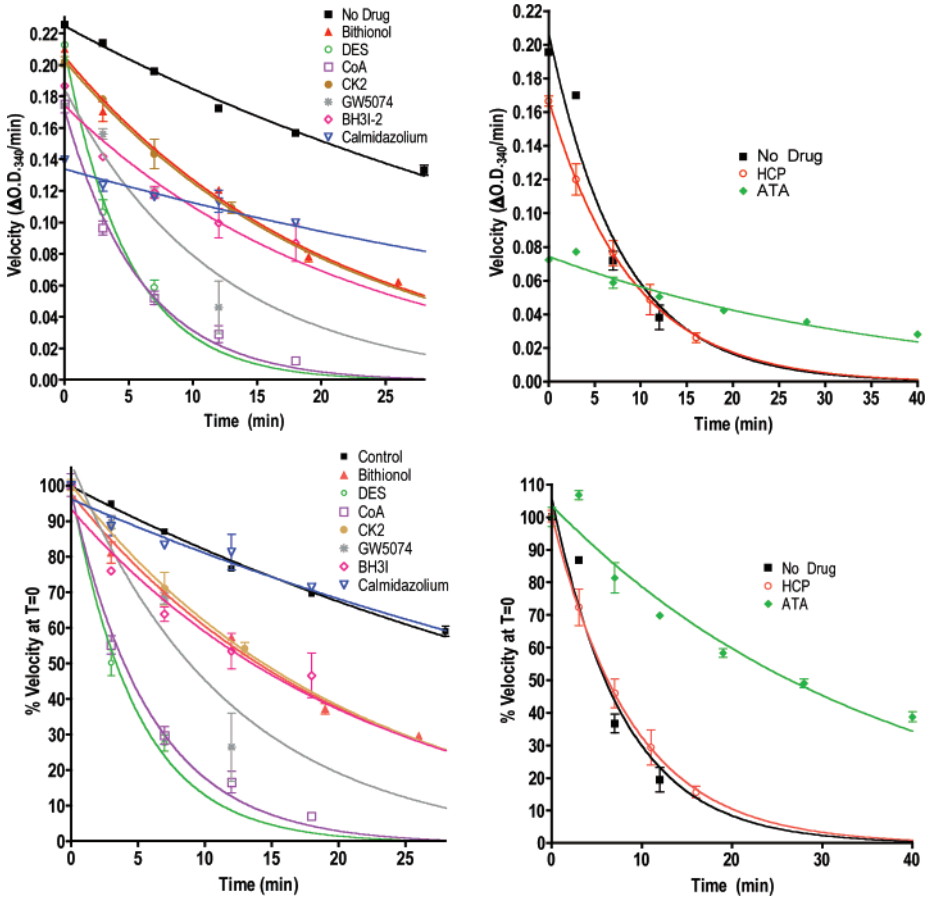

FIGURE 10: The effects of the inhibitors on GDH thermal stability. The top figures show the activity of the enzyme at various times at 50 °C (left) and 54° (right) in the presence of various compounds. Since there was some carryover inhibition due to the drug added during the incubation, the bottom two figures show the same data normalized to the velocity before the incubation at high temperature was initiated. The curves show the results of the linear-regression analysis using eq 7.

Table 5: The Effects of the Inhibitors on the Thermal Stability of GDH[a]

compound	rate (min^{-1})	R^2	half-life (min)	temp (°C)
no drug	0.020 (0.001)	0.99	34.5	50
bithionol	0.048 (0.002)	0.99	14.4	50
diethystilbestrol	0.202 (0.017)	0.98	3.4	50
palmitoyl CoA	0.169 (0.011)	0.99	4.1	50
CK2 inhibitor	0.048 (0.003)	0.98	14.4	50
GW5074	0.084 (0.016)	0.87	8.2	50
BH3I-2	0.046 (0.006)	0.90	15.0	50
calmidazolium	0.017 (0.031)	0.82	40.6	50
no drug	0.127 (0.019)	0.93	5.4	54
hexachlorophene	0.113 (0.007)	0.98	6.1	54
ATA	0.028 (0.002)	0.94	24.6	54

[a] This is a summary of the data shown in Figure 10 and fitted to eq 7.

two phenolic groups, are. This seems to suggest that two phenolic groups with this approximate spacing are a minimum requirement for activity. Owing to the rather diverse chemical nature and pharmaceutical activities of these compounds, it would not be surprising if these compounds bound to a number of sites and/or exerted their inhibitory effects on the enzyme in different ways.

Since GDH utilizes commonly found substrate, glutamate, and coenzymes, $NAD(P)^+$, it was essential to design the high throughput screen to avoid selection of substrate and coenzyme analogues. To that end, very high concentrations of both coenzyme and substrate were used during the screening. This proved to be efficacious in that none of the compounds subjected to detailed analysis exhibited signs of competitive inhibition.

Out of the compounds that were further studied, it is particularly interesting that most appear to affect the enzyme in a positively cooperative manner. This, in effect, causes a sudden and rapid increase in inhibition as the drug reached the apparent K_i. Interestingly, GW5074 and CK2 inhibitor did not fit this pattern. Indeed, GW5074 was accidentally tested twice under the name C-Raf1 inhibitor and consistently yielded the same Hill coefficient. In contrast, higher Hill coefficients are associated with the more hydrophobic compounds. Perhaps, these compounds are intercalating into the enzyme and this process is easier once several molecules have already bound. It is more difficult to interpret the ATA and BSB apparent cooperativity since these compounds tend to readily polymerize in solution.

Kinetic analysis of GDH is difficult because the enzyme does not exhibit classical Michaelis−Menten behavior in a number of aspects. In the oxidative deamination reaction, the GDH exhibits marked negative cooperativity with respect to coenzyme. While most of the previous steady-state kinetic analyses relied on interpretation of linearized rate data via Lineweaver−Burk plots, we have employed the Hill equation to better assess the mode of inhibition and possible effects on non-Michaelis−Menten kinetics such as substrate inhibition and negative cooperativity. From the results presented here, the data is well described by the mathematical models and represents a superior way to describe these complex

kinetic phenomena. The assay conditions for the high throughput screen were performed at very high glutamate and coenzyme concentrations to avoid identifying ligands that might mimic substrate and coenzyme. From these results (Figure 5 and Tables 2 and 3) it is apparent that this accomplished that goal. None of the compounds tested were apparently purely competitive inhibitors of the reaction. Further, none of the compounds eliminated the negative cooperativity or substrate inhibition observed in the oxidative deamination reaction. Interestingly, BSB and ATA are less efficacious at the very high glutamate concentrations where marked substrate inhibition occurs and cause a significant increase in the K_m for glutamate. This suggests that these inhibitors may act by interfering with the formation of the catalytic complex while compounds like hexachlorophene appear to enhance the formation of the catalytic (and likely abortive) complexes.

The effects of ADP on the various compounds clearly demonstrate that not all act via the same mechanism and likely bind to different locations on the enzyme. ADP exhibits complex kinetic effects on GDH (*18*). Essentially, ADP is most efficacious under conditions where product release is greatly inhibited by abortive complex formation. When conditions are such that there is weak binding of substrate/coenzyme, then ADP can actually inhibit the reaction (*18*). We suggested that ADP acts by binding behind the NAD binding domain and facilitating the opening of the catalytic cleft (Figure 1 and ref (*43*)). Similarly, ADP abrogation of inhibitor effects is complex and cannot always be ascribed to a direct competition. For example, we know that ADP (*43*) and GTP (*24*) bind to separate locations on GDH and yet are antagonists. ADP also reverses the effects of EGCG (*14*) and palmitoyl CoA (*44*), and yet genetically removal of the antenna (Figure 1) also eliminates ADP activation, GTP inhibition, and palmitoyl CoA inhibition (*44*) in spite of it not being directly involved in either GTP or ADP binding. With nearly all of the drugs, ADP is a highly efficacious antagonist except for GW5074, a known ATP/GTP analogue.

Therefore, putting all of the results together, there are apparently at least three general classes of compounds. The first group is best represented by GW5074. Unlike the other inhibitors described here, it does not affect the enzyme in an apparent positive cooperative manner, but like most of the other drugs, it does seem to somewhat accelerate thermal inactivation of the enzyme. Also unique to GW5074 is that it is a specific kinase inhibitor and one end has the general shape of a purine. The question, however, is whether it likely binds to the ADP site or to the GTP site? We know that GTP binding is heavily dominated by the triphosphate moiety as clearly demonstrated by the fact that GMP and GDP have little to no effect on the enzyme (*24*). GW5074 clearly does not have an obvious portion of the molecule that would mimic the triphosphate of GTP. In contrast to GTP, ADP binds to its site via extensive interactions with the purine ring (*43*), and we suggested that it activates via phosphate interactions with a lysine residue on the pivot helix (*44*). In a seeming paradox, we have shown that a second molecule of NADH also binds to the ADP site (*43*) and yet it has been suggested to inhibit the enzyme (*45*−*48*). Perhaps compounds like GW5074 bind to the ADP site and inhibit enzymatic activity in a manner akin to NADH, if NADH inhibition is indeed caused by binding to this site (*43*). The ED_{50} for ADP is more than 20 times higher than that for GW5074. Perhaps, under these conditions, ADP was not antagonistic to GW5074 since it was not able to effectively compete for binding. Circumstantial support for this possibility comes from the fact that GW5074 does not affect the apparent binding constant of ADP in the kinetic assays.

The second class of inhibitors is the large, polyphenolic structures represented by EGCG, ATA, and BSB. ATA interferes with protein/RNA interactions, and BSB interacts with amyloid polymers. The binding results clearly demonstrate that ATA and BSB interact in a highly specific manner with GDH as does the specificity of ECGG and ECG for GDH over EC and EGC. Both ATA and BSB show apparent cooperative inhibitory effects but not quite as strongly as do some of the smaller compounds such as hexachlorophene. Unlike GW5074, the effects of ATA, BSB, and EGCG (*14*) are strongly abrogated by ADP. It should also be noted that all three compounds form larger polymers in solution. At least for EGCG, it is known that the larger polymers also have inhibitory activity (*14*). We also know that at least EGCG can inhibit the HI/HA forms of GDH that have a nonfunctional GTP inhibition site and that EGCG requires the antenna for activity (*14*). The other interesting common feature of ATA and BSB is that the inhibition appears to be weaker at higher glutamate concentrations (Figure 6), suggesting that these compounds may affect the formation of the catalytic complex perhaps by interfering with the closing of the catalytic cleft. This could explain why ADP is such an effective antagonist since we have previously suggested that it acts by facilitating the opening of the catalytic cleft (*43*). Perhaps ATA stabilizes GDH against thermal denaturation by binding between the domains of this rather mobile enzyme.

The final class of compounds is represented by bithionol and hexachlorophene. Similar to ATA and BSB, these compounds appear to act in a cooperative manner (Table 1). Unlike ATA, BSB, and EGCG, these compounds do not form large polymers in solution and may be homologues of the previously identified inhibitor diethylstilbestrol (*49*). Common to the larger compounds, these have at least two aromatic rings. Notably, the single ring phenol, gallate (Figure 3), is inactive and yet has the anti-oxidative activity of EGCG. It is possible that these smaller compounds bind to the same or similar sites as ATA and BSB, but do so in a monovalent manner. It is not clear whether palmitoyl CoA belongs in this group, but like EGCG, the presence of the antenna is necessary for inhibition (*44*). Interestingly, suloctidil has a single aromatic group but has an aliphatic chain similar to palmitoyl CoA.

As has been shown in numerous studies over the past 40 years, GDH is an extremely complex enzyme with a network of allosteric regulation that is not readily dissected. Full understanding of how these various compounds inhibit GDH activity will more than likely require the structures of the enzyme/drug complexes, but such details will greatly elucidate the subunit communications associated with enzymatic catalysis and regulation.

ACKNOWLEDGMENT

The high throughput screening was performed using the facilities at the Broad Institute that is supported by Federal

funds from the National Cancer Institute's Initiative for Chemical Genetics, National Institutes of Health, under Contract No. N01-CO-12400. The content of this publication does not necessarily reflect the views or policies of the Department of Health and Human Services, nor does mention of trade names, commercial products or organizations imply endorsement by the U.S. Government.

REFERENCES

1. Brunhuber, N. M. W., and Blanchard, J. S. (1994) The biochemistry and enzymology of amino acid dehydrogenases, *Crit. Rev. Biochem. Mol. Biol. 29*, 415−567.
2. Sener, A., and Malaisse, W. J. (1980) L-leucine and a nonmetabolized analogue activate pancreatic islet glutamate dehydrogenase, *Nature 288*, 187−189.
3. Sener, A., Malaisse-Lagae, F., and Malaisse, W. J. (1981) Stimulation of pancreatic islet metabolism and insulin release by a nonmetabolizable amino acid, *Proc. Natl. Acad. Sci. U.S.A. 78*, 5460−5464.
4. Fahien, L. A., MacDonald, M. J., Kmiotek, E. H., Mertz, R. J., and Fahien, C. M. (1988) Regulation of insulin release by factors that also modify glutamate dehydrogenase, *J. Biol. Chem. 263*, 13610−13614.
5. Maechler, P., and Wollheim, C. B. (1999) Mitochondrial glutamate acts as a messenger in glucose-induced insulin exocytosis, *Nature 402*, 685−689.
6. Macdonald, M. J., and Fahien, L. A. (2000) Glutamate is not a messenger in insulin secretion, *J. Biol. Chem. 275*, 34025−34027.
7. Li, C., Najafi, H., Daikhin, Y., Nissim, I., Collins, H. W., Yudkoff, M., Matschinsky, F. M., and Stanley, C. A. (2003) Regulation of leucine stimulated insulin secretion and glutamine metabolism in isolated rat islets, *J. Biol. Chem. 278*, 2853−2858.
8. Li, C., Buettger, C., Kwagh, J., Matter, A., Daihkin, Y., Nissiam, I., Collins, H. W., Yudkoff, M., Stanley, C. A., and Matschinsky, F. M. (2004) A signaling role of glutamine in insulin secretion, *J. Biol. Chem. 279*, 13393−13401.
9. Stanley, C. A. (2000) The hyperinsulinism-hyperammonemia syndrome: gain-of-function mutations of glutamate dehydrogenase, in *Genetic Insights in Paediatric Endocrinology and Metabolism* (O'Rahilly, S., and Dunger, D. B., Eds.) pp 23−30, BioScientifica, Ltd, Bristol.
10. Stanley, C. A., Lieu, Y. K., Hsu, B. Y., Burlina, A. B., Greenberg, C. R., Hopwood, N. J., Perlman, K., Rich, B. H., Zammarchi, E., and Poncz, M. (1998) Hyperinsulinism and hyperammonemia in infants with regulatory mutations of the glutamate dehydrogenase gene, *N. Engl. J. Med. 338*, 1352−1357.
11. Stanley, C. A., Fang, J., Kutyna, K., Hsu, B. Y., Ming, J. E., Glaser, B., and Poncz, M. (2000) Molecular basis and characterization of the hyperinsulinism/hyperammonemia syndrome: predominance of mutations in exons 11 and 12 of the glutamate dehydrogenase gene. HI/HA Contributing Investigators, *Diabetes 49*, 667−673.
12. MacMullen, C., Fang, J., Hsu, B. Y. L., Kelly, A., deLonlay-Debeney, P., Saudubray, J. M., Ganguly, A., Smith, T. J., and Stanley, C. A. (2001) The Hyperinsulinism/hyperammonemia Contributing Investigators. Hyperinsulinism/hyperammonemia syndrome in children with regulatory mutations in the inhibitory guanosine triphosphate-binding domain of glutamate dehydrogenase, *J. Clin. Endocrinol. Metab. 86*, 1782−1787.
13. Hsu, B. Y., Kelly, A., Thornton, P. S., Greenberg, C. R., Dilling, L. A., and Stanley, C. A. (2001) Protein-sensitive and fasting hypoglycemia in children with the hyperinsulinism/hyperammonemia syndrome, *J. Pediatr. 138*, 383−389.
14. Li, C., Allen, A., Kwagh, K., Doliba, N. M., Qin, W., Najafi, H., Collins, H. W., Matschinsky, F. M., Stanley, C. A., and Smith, T. J. (2006) Green Tea Polyphenols Modulate Insulin Secretion by Inhibiting Glutamate Dehydrogenase, *J. Biol. Chem 2006*, 10214−10221.
15. Hill, A. V. (1910) The possible effects of the aggregation of the molecules of haemoglobin on its dissociation curves, *J. Physiol. (London) 40*, iv−vii.
16. Vazquez, J. A., Bonzalez, M. P., and Murado, M. A. (2003) Substrate inhibition of Pediococcus acidilactici by glucose on a waste medium. Simulations and experimental results, *Lett. Appl. Mirobiol. 37*, 365−369.
17. Sanner, T. (1975) Formation of transient complexes in the glutamate dehydrogenase catalyzed reaction, *Biochemistry 14*, 5094−5098.
18. Bailey, J. S., Bell, E. T., and Bell, J. E. (1982) Regulation of bovine glutamate dehydrogenase, *J. Biol. Chem. 257*, 5579−5583.
19. Swillens, S. (1995) Interpretation of binding curves obtained with high receptor concentrations: practical aid for computer analysis, *Mol. Pharm. 47*, 1197−1203.
20. Dalziel, K., and Engel, P. C. (1968) Antagonistic homotropic interactions as a possible explanation of coenzyme activation of glutamate dehydrogenase, *FEBS Lett. 1*, 349−352.
21. Engel, P., and Dalziel, K. (1969) Kinetic studies of glutamate dehydrogenase with glutamate and norvaline as substrates, *Biochem. J. 115*, 621−631.
22. Bell, J. E., and Dalziel, K. (1973) A conformational transition of the oligomer of glutamate dehydrogenase induced by half-saturation with NAD^+ or $NADP^+$, *Biochim. Biophys. Acta 309*, 237−242.
23. Bell, E. T., LiMuti, C., Renz, C. L., and Bell, J. E. (1985) Negative co-operativity in glutamate dehydrogenase. Involvement of the 2-position in the induction of conformational changes, *Biochem. J. 225*, 209−217.
24. Smith, T. J., Peterson, P. E., Schmidt, T., Fang, J., and Stanley, C. (2001) Structures of bovine glutamate dehydrogenase complexes elucidate the mechanism of purine regulation, *J. Mol. Biol. 307*, 707−720.
25. Smith, T. J., Schmidt, T., Fang, J., Wu, J., Siuzdak, G., and Stanley, C. A. (2002) The structure of apo human glutamate dehydrogenase details subunit communication and allostery, *J. Mol. Biol. 318*, 765−777.
26. Lewis, J. K., Bothner, B., Smith, T. J., and Siuzdak, G. (1998) Antiviral agent blocks breathing of the common cold virus, *Proc. Natl. Acad. Sci. 95*, 6774−6778.
27. Reisdorph, N., Thomas, J., Katpally, U., Chase, E., Harris, K., Siuzdak, G., and Smith, T. J. (2003) Human rhinovirus capsid dynamics is controlled by canyon flexibility, *Virology 314*, 34−44.
28. Hallick, R. B., Chelm, B. K., Gray, P. W., and Orozco, E. M. J. (1977) Use of aurintricarboxylic acid as an inhibitor of nucleases during nucleic acid isolation, *Nucleic Acids Res. 4*, 3055−3064.
29. Benchokroun, Y., Couprie, J., and Larsen, A. K. (1995) Aurintricarboxylic acid, a putative inhibitor of apoptosis, is a potent inhibitor of DNA topoisomerase II in Vitro and in Chinese hamster fibrosarcoma cells, *Biochem. Pharmacol. 49*, 305−313.
30. Gonzalez, R. G., Haxo, R. S., and Schleich, T. (1980) Mechanism of action of polymeric aurintricarboxylic acid, a potent inhibitor of protein−nucleic acid interactions, *Biochemistry 19*, 4299−4303.
31. Sarno, S., Reddy, H., Meggio, F., Ruzzene, M., Davies, S. P., Donella-Deana, A., Shugar, D., and Pinna, L. A. (2001) Selectivity of 4,5,6,7-tetrabromobenzotriazole, an ATP site-directed inhibitor of protein kinase CK2 ('casein kinase-2'), *FEBS Lett. 496*, 44−48.
32. Skovronsky, D. M., Zhang, B., Kung, M.-P., Kung, H. F., Trojanowski, J. Q., and Lee, V. M.-Y. (2000) In vivo detection of amyloid plaques in a mouse model of Alzheimer's disease, *Proc. Natl. Acad. Sci. U.S.A. 97*, 7609−7614.
33. Ishikawa, K., Doh-ura, K., Kudo, Y., Nishida, N., Murakami-Kubo, I., Ando, Y., Sawada, T., and Iwaki, T. (2004) Amyloid imaging probes are useful for detection of prion plaques and treatment of transmissible spongiform encephalopathies, *J. Gen. Virol. 85*, 1785−1790.
34. Degterev, A., Lugovskoy, A., Cardone, M., Mulley, B., Wagner, G., Mitchison, T., and Yuan, J. (2001) Identification of small-molecule inhibitors of interaction between BH3 domain and Bcl-xL, *Nat. Cell Biol. 3*, 173−182.
35. Wang, Y., and Rosenberg, R. L. (1991) Ethaverine, a derivative of papaverine, inhibits cardiac L-type calcium channels., *Mol. Pharm. 40*, 750−755.
36. Calderon, P., van Dorsser, W., Geöcze von Szendroi, K., De Mey, J. G., and Roba, J. (1986) In vitro vasorelaxing activity of suloctidil, *Arch. Int. Pharmacodyn. Ther. 284*, 101−113.
37. Piccioni, F., Roman, B. R., Fischbeck, K. H., and Taylor, J. P. (2004) A screen for drugs that protect against the cytotoxicity of polyglutamine-expanded androgen receptor, *Hum. Mol. Genet. 13*, 437−446.
38. Kindmark, H., Köhler, M., Gerwins, P., Larsson, O., Khan, A., Wahl, M. A., and Berggren, P. O. (1994) The imidazoline derivative calmidazolium inhibits voltage-gated Ca(2+)-channels

and insulin release but has no effect on the phospholipase C system in insulin producing RINm5F-cells, *Biosci. Rep. 14*, 145−158.
39. Lamers, J. M., and Stinis, J. T. (1983) Inhibition of Ca2+-dependent protein kinase and Ca2+/Mg2+-ATPase in cardiac sarcolemma by the anti-calmodulin drug calmidazolium, *Cell Calcium 4*, 281−294.
40. Fuller, R. W., and Snoddy, H. D. (1979) The effects of metergoline and other serotonin receptor antagonists on serum corticosterone in rats, *Endocrinology 105*, 923−928.
41. Miller, K. J., King, A., Demchyshyn, L., Niznik, H., and Teitler, M. (1992) Agonist activity of sumatriptan and metergoline at the human 5-HT1Db receptor: Further evidence for a role of the 5-HT1D receptor in the action of sumatriptan, *Eur. J. Pharmacol. 227*, 99−102.
42. Dodds, E. C., Goldberg, L., Lawson, W., and Robinson, R. (1938) Estrogenic activity of certain synthetic compounds, *Nature 141*, 247−248.
43. Banerjee, S., Schmidt, T., Fang, J., Stanley, C. A., and Smith, T. J. (2003) Structural studies on ADP activation of mammalian glutamate dehydrogenase and the evolution of regulation, *Biochemistry 42*, 3446−3456.
44. Allen, A., Kwagh, J., Fang, J., Stanley, C. A., and Smith, T. J. (2004) Evolution of glutamate dehydrogenase regulation of insulin homeostasis is an example of molecular exaptation, *Biochemistry 43*, 14431−14443.
45. Koberstein, R., and Sund, H. (1973) The influence of ADP, GTP and L-glutamate on the binding of the reduced coenzyme to beef-liver glutamate dehydrogenase, *Eur. J. Biochem. 36*, 545−552.
46. Malcolm, A. D. B. (1972) Coenzyme binding to glutamate dehydrgenase. A study by relaxation kinetics, *Eur. J. Biochem. 27*, 453−461.
47. Saradambal, K. V., Bednar, A. R., and Colman, R. F. (1981) Lysine and tyrosine in the NADH inhibitory site of bovine liver glutamate dehydrogenase, *J. Biol. Chem. 256*, 11866−11872.
48. Schmidt, J. A., and Colman, R. F. (1984) Identification of the lysine and tyrosine peptides labeled by 5′-*p*-fluorosulfonylbenzoyladenosine in the NADH inhibitory site of glutamate dehydrogenase, *J. Biol. Chem. 259*, 14515−14519.
49. Tomkins, G. M., Yielding, K. L., and Curran, J. F. (1962) The influence of diethylstilbestrol and adenosine diphosphate on pyridine nucleotide coenzyme binding by glutamic dehydrogenase, *J. Biol. Chem. 237*, 1704−1708.
50. Lackey, K., Cory, M., Davis, R., Frye, S. V., Harris, P. A., Hunter, R. N., Jung, D. K., McDonald, O. B., McNutt, R. W., Peel, M. R., Rutkowske, R. D., Veal, J. M., and Wood, E. R. (2000) The discovery of potent cRaf1 kinase inhibitors, *Bioorg. Med. Chem. Lett. 10*, 223−226.
51. Szyszka, R., Grankowski, N., Felczak, K., and D., S. (1995) Halogenated benzimidazoles and benzotriazoles as selective inhibitors of protein kinases CK I and CK II from Saccharomyces cerevisiae and other sources, *Biochem. Biophys. Res. Commun. 208*, 418−424.
52. Fischer, T. H., Campbell, K. P., and White, G. C. (1987) An investigation of functional similarities between the sarcoplasmic reticulum and platelet calcium-dependent adenosinetriphosphatases with the inhibitors quercetin and calmidazolium, *Biochemistry 26*, 8024−8030.
53. Chatelain, P., Demol, D., and Roba, J. (1984) Inhibition by suloctidil of [3H] nitrendipine binding to cerebral cortex membranes, *Biochem. Pharmacol. 33*, 1099−1103.

BI7018783